Research Square

Preprints are preliminary reports that have not undergone peer review.
They should not be considered conclusive, used to inform clinical practice,
or referenced by the media as validated information.

Resolution of Inflammation by 17(S)-HDHA Confers Neuroprotection After Ischemic Spinal Cord Injury

Renato Rozental

renato.rozental@fiocruz.br

Fundação Oswaldo Cruz (Fiocruz) https://orcid.org/0000-0003-0092-6076

Caio Perret

https://orcid.org/0000-0003-1769-2034

Tagore de Morais

Chiara Pimentel

Raphael Bertani

Rene Beleboni

Fabio Nogueira

Karsten Gronert

Article

Keywords: spinal cord injury (SCI), ischemic spinal cord injury (iSCI), 17(S) hydroxyl-docosahexaenoic-acid (17(S)-HDHA), connexin43 (Cx43), Specialized Pro-Resolving Mediators (SPMs), inflammation, cerebrospinal fluid (CSF).

Posted Date: November 23rd, 2026

DOI: https://doi.org/10.21203/rs.3.rs-11274143/v1

License: This work is licensed under a Creative Commons Attribution 4.0 International License.
Read Full License

Additional Declarations: There is no duality of interest

MS #2: Mechanism and therapeutic targeting (proof of concept)
back-to-back submission

"Resolution of Inflammation by 17(S)-HDHA Confers Neuroprotection After Ischemic Spinal Cord Injury"

[1,2]Caio Perret¶, [1]Tagore G. de Morais¶, [1]Chiara D. Pimentel, [2]Raphael M. Bertani, [3]Rene O. Beleboni, [4]Fabio C.S. Nogueira, [5]Karsten Gronert, [1,6,7]Renato Rozental*.

¶ contributed equally to this work

[1]Instituto de Ciências Biomédicas, CCS, Universidade Federal do Rio de Janeiro, RJ, 21941-902, Brazil.
[2]Hospital Municipal Miguel Couto, Rio de Janeiro, RJ, 22430-160, Brazil.
[3]Unidade de Biotecnologia, Universidade de Ribeirão Preto, UNAERP, São Paulo, 14096-900, Brazil.
[4]Instituto de Quimica, Universidade Federal do Rio de Janeiro, RJ, 21941-598, Brazil.
[5]Herbert Wertheim School of Optometry & Vision Science, University of California, Berkeley, CA, 94720-2020, USA.
[6]Dept Neuroscience, Albert Einstein Coll Medicine, Bronx, NY, 10461, USA.
[7]Centro Desenvolvimento Tecnológico (CDTS) and Instituto Oswaldo Cruz (IOC), FIOCRUZ, Rio de Janeiro, 21040-361, Brazil

*Corresponding author:
Renato Rozental, *MD, PhD*
renato.rozental@fiocruz.br

Fundação Oswaldo Cruz - FIOCRUZ
Centro de Desenvolvimento Tecnológico em Saúde (*CDTS*)
Térreo – r. 06
Av. Brasil 4365, Campus Manguinhos
Manguinhos, Rio de Janeiro, 21040-360
Brasil

Keywords: spinal cord injury (SCI); ischemic spinal cord injury (iSCI); 17(S) hydroxyl-docosahexaenoic-acid (17(S)-HDHA); connexin43 (Cx43); Specialized Pro-Resolving Mediators (SPMs); inflammation; cerebrospinal fluid (CSF).

ILLUSTRATIONS:

- 3 MAIN FIGURES (figure legends appear after the References section)
- 2 SUPPLEMENTARY FIGURES (*Supporting Information*)
- 1 SUPPLEMENTARY TABLE (*Supporting Information*)

ABSTRACT

Study Design: Animal study. Female Sprague-Dawley rats.

Objectives: To determine whether pharmacological augmentation of the endogenous DHA-derived inflammatory-resolution pathway with 17(S)-hydroxydocosahexaenoic acid [17(S)-HDHA] limits secondary tissue degeneration and preserves neural function following ischemic spinal cord injury (SCI).

Setting: Brazil and USA.

Methods: In an anesthesia-free rat model of ischemic SCI, lipidomic analyses characterized DHA-derived lipid mediators in cerebrospinal fluid (CSF) from rats and patients with SCI. Rats received intravenous 17(S)-HDHA from paralysis onset through five days. Spinal cord (SC) tissue integrity, macrophage/microglial activation, reactive astrogliosis, connexin-43 (Cx43) expression, spinal motor network function, and systemic toxicity were evaluated.

Results: 17-HDHA was detected in CSF from both rats and patients with SCI, whereas downstream specialized pro-resolving mediators were not detected. Intravenous 17(S)-HDHA rapidly reached rat SC tissue without detectable acute systemic toxicity or corticosteroid-associated metabolic disturbances. Treatment reduced macrophage/microglial activation and reactive astrogliosis, attenuated SC atrophy and tissue degeneration, and preserved spinal motor network function, as demonstrated by improved electromyographic activity. These effects were accompanied by reduced Cx43 expression.

Conclusions: 17-HDHA is an early endogenous component of inflammatory resolution after ischemic SCI, but endogenous activation appears insufficient to prevent secondary degeneration. Therapeutic augmentation with 17(S)-HDHA limits neuroinflammation and tissue degeneration while preserving spinal motor network function, providing a complementary strategy for neuroprotection after ischemic SCI.

Sponsorship: FAPERJ; Brazilian Ministry of Health; and New York State SCI Research.

INTRODUCTION

Ischemic spinal cord injury (iSCI) initiates a rapidly evolving secondary injury cascade characterized by progressive neuroinflammation, tissue degeneration, and neurological dysfunction[1]. In the companion study, using an anesthesia-free model of ischemic SCI induced by maximal electroshock seizures (MES), we demonstrated that inflammatory and resolution programs are activated concurrently within the first 24 h after injury (**Fig. S1**). Despite induction of the DHA-lipoxygenase pathway and detectable endogenous production of 17-hydroxy-docosahexaenoic acid (17-HDHA), downstream specialized pro-resolving mediator (SPM) biosynthesis remained incomplete and was accompanied by suppression of astrocytic pathways involved in lipid mobilization and metabolism. These findings suggested that acute ischemic SCI is characterized not simply by excessive inflammation, but by an early failure to mount an effective endogenous resolution response.

Specialized pro-resolving mediators (SPMs) are bioactive lipid mediators derived from polyunsaturated fatty acids (PUFAs) (**Fig. S2**), including lipoxins, resolvins, protectins, and maresins, that actively coordinate the termination of inflammation and restoration of tissue homeostasis[2-4]. Unlike conventional anti-inflammatory therapies, which broadly suppress immune responses, SPMs promote resolution through regulation of leukocyte trafficking, enhancement of efferocytosis, attenuation of inflammatory signaling, and stimulation of tissues repair programs[5]. Among these pathways, the docosahexaenoic acid (DHA)-derived metabolite 17-HDHA occupies a central position as a biosynthetic intermediate for D-series resolvins and neuroprotectins and has been associated with potent neuroprotective and immunomodulatory effects in experimental models of CNS injury[2,6,7]. Inadequate, delayed, or insufficient production of SPMs has been implicated in the persistence of chronic inflammation and progressive tissue injury across a range of neurological and systemic disorders[2,4,8].

Previous studies performed in anesthetized SCI models reported delayed activation of resolution pathways, with substantial increases in pathway markers such as 17-HDHA and 14-HDHA emerging only during later phases of injury[9]**.** In contrast, our study identified endogenous 17-HDHA production within the first 24 h after ischemic SCI, indicating that pro-inflammatory and pro-resolving programs are engaged much earlier than previously appreciated. However, the transient nature of this response and the absence of downstream SPM generation suggested that endogenous resolution mechanisms are insufficient to counterbalance inflammatory amplification during the acute phase of injury.

Notably, whether resolution-oriented lipid mediators regulate connexin (Cx) signaling during the acute phase of SCI remains largely unexplored. Connexins are the structural proteins that assemble into gap junction (GJ) channels and hemichannels[10-12], both of which have emerged as important regulators of neuroinflammation[12-15]**.** Among these, connexin43 (Cx43), the predominant connexin expressed by astrocytes and an inducible component of signaling networks in innate immune cells, including macrophages and microglia, is markedly upregulated in response to inflammatory stimuli and CNS injury[11,13,17-18]. Under pathological conditions, Cx43 hemichannels open to the extracellular

space, facilitating the release of ATP, glutamate, cytokines, and other signaling molecules that activate purinergic and inflammatory pathways, thereby amplifying cytokine production, neuroinflammation, and propagation of secondary injury[12,18,19-22.] In parallel, GJs facilitate direct intercellular communication and may propagate deleterious bystander signals, extending inflammatory and metabolic dysfunction beyond the primary lesion site[13,16,19,23]. Thus, Cx43-dependent signaling may establish a feed-forward mechanism that sustains and amplifies secondary injury after SCI. Whether restoration of endogenous resolution pathways can modulate this process remains unknown, raising the possibility that pro-resolving mediators may confer neuroprotection not only by attenuating inflammatory activation but also by limiting Cx-dependent propagation of tissue damage.

Based on these observations, we hypothesized that therapeutic augmentation of this early endogenous resolution signal could restore key components of the resolution program and limit secondary injury progression. To test this hypothesis, we investigated the effects of systemic 17(S)-HDHA administration in the acute phase of ischemic SCI. Using complementary histological, molecular, metabolic, and electrophysiological analyses, we demonstrate that 17(S)-HDHA attenuates inflammatory cell activation, reduces tissue damage, modulates connexin-43 (Cx43) signaling, preserves motor network organization, and improves functional outcomes. Together, these findings establish 17-HDHA as a therapeutically actionable regulator of inflammatory resolution and provide proof-of-concept that resolution pharmacology represents a viable strategy for neuroprotection after acute ischemic SCI.

MATERIAL AND METHODS

Experimental design and 17(S)-HDHA treatment

Adult Sprague–Dawley rats underwent ischemic SCI induced by the repeated transauricular maximal electroshock seizure (MES) paradigm performed between gestational days 4 and 21, as described in the companion animal model manuscript. Briefly, awake animals received transauricular MES stimulation through ear-clip electrodes delivering square-wave pulses (120 V, 50 Hz, 50% duty cycle, 2 s), producing a reproducible thoracolumbar ischemic SCI. Detailed experimental design, animals and group allocation are described in ***SI Materials and Methods***.

Immediately following the onset of hindlimb paralysis, animals underwent neurological examination (NE) to determine the neurological level of injury before being assigned to receive either 17(S)-HDHA (7 µg in 100 µL sterile saline, intravenous) or vehicle (100 µL of 0.9% sterile saline). The selected dose of 17(S)-HDHA exceeded the threshold previously reported to elicit biological activity of specialized pro-resolving mediators (SPMs) within the central nervous system despite an intact blood–brain barrier[9,24,25]**.** The initial dose was administered 10–15 min after paralysis onset, followed by two additional intravenous injections at 48-h intervals (days 3 and 5), resulting in three administrations over the 5-day experimental period. Animals were allocated prospectively to predefined experimental endpoints, including magnetic

resonance imaging (MRI), electromyography (EMG), lipidomic, transcriptomic, proteomic, immunoblotting, histopathological, immunohistochemical, and three-dimensional morphometric analyses, according to the study design (**Fig. S1**).

For the purposes of this study, the hyperacute phase was defined as the first 24 h after SCI, during which inflammatory and endogenous pro-resolving pathways are initiated, and the trajectory of secondary injury is established. The acute phase was defined as the subsequent 5-day period after injury, characterized by amplification of the inflammatory response, glial activation, progressive secondary tissue degeneration, and the emergence of functional deficits.

Preparation of 17(S)-HDHA, spinal cord tissue penetration and metabolic safety under physiological conditions

17(S)-HDHA was prepared enzymatically from docosahexaenoic acid (DHA) and purified by reverse-phase high-performance liquid chromatography (RP-HPLC) as previously described[6,26]. Purified 17(S)-HDHA (purity ≥98%) was stored at −80 °C until use and administered in the therapeutic studies described above. See details for synthesis, purification, chromatographic characterization, and quality control are provided in ***SI Materials and Methods***.

To determine whether systemically administered 17(S)-HDHA reaches SC tissue under physiological conditions, an independent cohort of non-MES-stimulated adult rats was anesthetized using a multimodal protocol consisting of inhalational sevoflurane and xylazine (5 mg/kg, i.p.). Animals received a single intravenous injection of deuterium-labelled 17-HDHA (d5-17-HDHA; 200 ng in 300 µL sterile 0.9% saline; Cayman Chemical, Ann Arbor, MI, USA), unlabelled 17-HDHA (200 ng in 300 µL sterile 0.9% saline), or vehicle (0.9% sterile saline) (n = 3 per group). Intravenous administration was selected to facilitate rapid systemic distribution and assess the acute biodistribution of the compound following bolus delivery. Forty-five minutes later, animals were euthanized, the thoracolumbar SC (T8–T12) was rapidly dissected, weighed, and processed for lipid extraction. Lipid mediators were isolated by solid-phase extraction and analyzed by reverse-phase liquid chromatography–tandem mass spectrometry (LC–MS/MS) to detect and quantify d5-17-HDHA within SC tissue. Authentic standards of 17-HDHA, d5-17-HDHA, 14-HDHA, and 7-HDHA (Cayman Chemical) were used for chromatographic identification and quantification. Detailed analytical procedures and LC–MS/MS conditions are described in the ***SI Materials and Methods***.

To evaluate the systemic metabolic safety of 17(S)-HDHA, a second independent cohort of non-MES-stimulated rats received a single intravenous bolus of either 17(S)-HDHA, methylprednisolone sodium succinate (1 mg/kg), or vehicle (0.9% sterile saline) (n = 6 per group). Blood samples were collected immediately before treatment and 24 h after administration for measurement of serum glucose and electrolyte concentrations (Na^+, K^+, Ca^{2+}, and Mg^{2+}) using an automated biochemical analyzer (ChemWell®, Labtest, Brazil). Serum biochemical data were analyzed using one-way analysis of variance (ANOVA) followed by Tukey's multiple-comparisons test in GraphPad Prism (version 9.0; GraphPad Software). A two-sided $P < 0.05$ was considered statistically significant. Additional methodological details are provided in the ***SI Materials and Methods***.

Tissue collection, histology and immunohistochemistry. Rats were anesthetized and transcardially perfused with 4% paraformaldehyde (PFA). SC were dissected, post-fixed overnight in 4% PFA, processed for paraffin embedding, and sectioned transversely at 10 µm thickness using a rotary microtome. Sections were stained with hematoxylin and eosin (H&E) for histopathological evaluation or processed for immunohistochemistry. Histological analyses were performed using four animals per group (control, MES-stimulated non-paralyzed, and MES-stimulated paralyzed rats) at 24 h and 5 days after injury.

Primary antibodies included anti-glial fibrillary acidic protein (GFAP; 1:500, Invitrogen), anti-CD11b (1:1,500, eBioscience), and anti-NeuN (1:5,000, Merck Millipore). Cell nuclei were counterstained with DAPI (1:1,500, Merck Millipore). See ***SI Materials and Methods*** *for details*.

Three-dimensional Spinal Cord Reconstruction and Lesion Volumetry. Volumetric analyses at day 5 were performed using five animals each in the control and MES-stimulated non-paralyzed groups and four animals in the MES-stimulated paralyzed group. Approximately 300 consecutive transverse sections (10 µm thick) spanning the T8–T12 SC segments were collected from each animal. Every twentieth section, corresponding to 200-µm intervals, was selected for three-dimensional (3D) reconstruction and quantitative lesion volumetry. Tissue contours and lesion boundaries were manually segmented by two independent investigators blinded to experimental group. Three-dimensional reconstructions were generated using Neurolucida® and Neurolucida Explorer® (MBF Bioscience, Williston, VT, USA). Lesion volume was estimated by volumetric integration of segmented areas of tissue loss across the sampled sections. Vacuolar degeneration was evaluated qualitatively but was not included in the volumetric analysis. Detailed procedures for tissue processing, image reconstruction, segmentation, volumetric calculations, and statistical analyses are provided in the **Supplementary Information Materials and Methods**.

Real-Time Quantitative PCR (RT-qPCR). RNA was isolated from SC samples obtained from three control and three paralyzed animals using TRIzol reagent (Invitrogen, Carlsbad, CA, USA) and from primary cultured astrocytes using the Absolute RNA® Miniprep Kit (Stratagene, La Jolla, CA, USA). Astrocyte experiments comprised three independent experiments, with two replicates per condition. RNA integrity was assessed by agarose gel electrophoresis, and RNA concentration was determined spectrophotometrically. RNA was reverse-transcribed using the SuperScript III First-Strand Synthesis System (Invitrogen). Rat leukocyte 12/15-LOX (Alox15) was amplified using established nucleotide primers[27]; sense 5'-GGCCCCGGAGACCAAGGAT-3' and antisense 5'-GCCGCCGCCACATTCAGG-3'. Specific nucleotide primers for rat reference genes (ubiquitin C, GAPDH, β-actin) were selected from the Real-Time PCR Data Base (medgen.ugent.be/rtprimerdb) and verified in the NIH Genbank®: Real-time PCR was performed using Brilliant SYBR Green QPCR Master Mix (Stratagene) and an MX3000 QPCR System (Stratagene). All amplifications were run in duplicates and amplification efficiencies for each primer pair were established. Comparative quantitation of gene expression was determined by MXPro analytical software (Stratagene).

Lipid Autacoids Analyses. Eicosanoids and DHA products were analyzed employing RP-HPLC and capillary GC/MS analysis as previously described[28,29]. In brief, analysis was performed with an Agilent 1100 series high performance liquid chromatography (HPLC) system (Agilent Technologies, Palo Alto, CA). Samples were injected in mobile phase and eluted on a Luna C18-2 minibore column (Phenomenex, Torrance, CA). Collected UV data were analyzed by LC 3D ChemStation software (Agilent Technologies).

GC/MS analysis was performed as in[26,28,] with a 6890N Gas Chromatography (GC) System with a HP5MS cross-linked ME siloxane column and a 5973N Mass Selective Detector (Agilent Technologies). For selected samples, HPLC fractions that correspond to established retention times of synthetic 17-HDHA were collected and derivatized to generate PFB esters and TMS ether derivatives and 10-1000 pg were injected in 2 µl iso-octane for GC/MS analysis.

For endogenous product analysis, frozen SC samples were homogenized (4^{o}C) in 100% MeOH containing PGB_2 (50 ng) as an internal standard for recovery and extracted by a C18 solid phase as previously detailed[29]. Methyl format fractions were taken to dryness under a gentle stream of nitrogen and resuspended in MeOH (100 µl) and stored at -80^{0}C.

Synthetic standards for 12-HETE, 15-HETE, 5-HETE, 17-HDHA, 14-HDHA, 7-HDHA were purchased from Cayman Chemical (Ann Arbor, MI). 17S-hydroxy-DHA for biological assays was prepared by incubation of DHA (Caymen Chemical) and soybean LOX (Type IV, Sigma). Each reaction condition used was optimized as previously described[6,26]. Reactions were terminated by acidification, extracted and 17S-HDHA isolated by RP-HPLC using a Beckman Coulter Ultrasphere column (4.6x250 mm, 5µm, Phenomenex, Torrance, CA). Physical criteria for identification such as HPLC retention times, specific UV chromophores, as well as GC/MS and LC/MS major and signature ions have been established for 17*S*-HDHA[6,24,26,28]. RP-HPLC purified 17H-DHA (2-4 mM stock, purity ≥ 98%) was stored in 100% ETOH at -80^{o}C. Endogenous arachidonic acid LOX products such as 12*S*-HETE, 15*S*-HETE, 5*S*-HETE as well as 14*S*-HDHA, 7*S*-HDHA and 4*S*-HDHA, which exhibit similar UV and MS characteristics, had distinct retention times in our HPLC system and did not coelute with 17*S*-HDHA.

Preparation and administration of 17(S)-HDHA and lipid mediator analysis. 17(S)-HDHA was synthesized enzymatically from docosahexaenoic acid (DHA) and purified by reverse-phase high-performance liquid chromatography (RP-HPLC) as previously described[6,24,26]. Product identity and purity were confirmed by chromatographic and mass spectrometric analyses using established physical criteria[6,24,26,28]. Animals received an intravenous bolus of 17(S)-HDHA (7 µg in 100 µL saline) via the tail vein within 15–20 min after the onset of paralysis, followed by repeat administration every other day until day 5 post-injury. The dose was selected based on previous studies demonstrating the biological activity of specialized pro-resolving mediators following systemic administration[24,25] and their neuroprotective efficacy after SCI[9].

Endogenous lipid mediators were quantified from SC tissue extracts by solid-phase extraction followed by RP-HPLC and lipidomic analyses using validated synthetic standards and internal recovery controls, as previously described[6,24,26,28]. Detailed protocols for 17(S)-HDHA synthesis, purification, quality control, lipid extraction, chromatographic separation, and lipid mediator identification are provided in ***SI***.

Hindlimb Vector Electromyographic (VEMG) recordings.

Intramuscular hindlimb vector electromyography (VEMG) was performed to assess spinal motor unit organization in uninjured control, vehicle-treated, and 17(S)-HDHA-treated rats using quadrifilar needle electrodes and Precision Decomposition analysis, as previously described[30,31]. Electrophysiological recordings were obtained from six animals (n = 2 per experimental group), with two to three recordings acquired per animal to confirm reproducibility. Because repeated recordings from the same animal are not statistically independent, each animal was considered the experimental unit. VEMG was used as a complementary physiological assessment of spinal motor circuit organization alongside behavioral, histopathological, and molecular analyses. *See* ***SI Materials and Methods*** *for* details.

Exploratory Serum Biochemistry and Metabolic Safety Assessment.

To explore the systemic metabolic safety of 17(S)-HDHA, an independent cohort was used for serum biochemical analyses. Animals were randomly assigned to three groups (n = 6 per group): vehicle-treated controls receiving a single intravenous bolus of 0.9% sterile saline, 17(S)-HDHA-treated animals receiving a single intravenous bolus, or methylprednisolone-treated animals receiving a single intravenous bolus of methylprednisolone (1 mg/kg), which served as a reference treatment because of its well-established association with corticosteroid-induced metabolic disturbances after SCI.

Blood samples were collected immediately before treatment administration and again over a 24-h observation period for routine serum biochemical analyses. Major biochemical analytes, including glucose, sodium (Na^+), potassium (K^+), calcium (Ca^{2+}), and magnesium (Mg^{2+}), were quantified using standard clinical laboratory methods. Emphasis was placed on blood glucose measurements to determine whether a single systemic administration of 17(S)-HDHA induced alterations in glycemia homeostasis comparable to those reported following corticosteroid treatment. Serum biochemical profiles of the 17(S)-HDHA-treated animals were compared with those of vehicle- and methylprednisolone-treated groups to provide an exploratory assessment of the systemic metabolic safety of 17(S)-HDHA.

Spinal Cord Tissue Penetration of Systemically Administered 17(S)-HDHA

To determine whether systemically administered 17(S)-HDHA reaches SC tissue, animals were randomly assigned to three groups (n = 3 per group). All animals were anesthetized and received a single intravenous (IV) bolus of either sterile 0.9% saline (vehicle control), unlabeled 17(S)-HDHA, or deuterium-labeled 17-HDHA (d_5-17-HDHA; 200 ng in 300 µL sterile saline). The dose and administration volume were matched between the unlabeled and deuterium-labeled 17-HDHA groups. Animals were euthanized 45 min after administration,

and thoracolumbar SC tissue was rapidly dissected for lipid extraction. Lipids were isolated by solid-phase extraction and analyzed by reverse-phase liquid chromatography–tandem mass spectrometry (LC–MS/MS) to detect d_5-17-HDHA. Compound identification was based on its characteristic chromatographic and mass spectrometric signature. Detection of d_5-17-HDHA in SC tissue was interpreted as evidence that systemically administered 17-HDHA reached the tissue within 45 min of administration.

Statistics analysis

General Statistical Analysis

Quantitative data are presented as mean ± standard deviation (SD). Descriptive and statistical analyses were performed using Microsoft Excel (Microsoft Corporation) or GraphPad Prism (GraphPad Software, San Diego, CA, USA), as appropriate. Comparisons between two groups were performed using Student's *t*-test, whereas comparisons among multiple groups were performed using one-way analysis of variance (ANOVA), as appropriate. The type of *t*-test (paired or unpaired), the use of one- or two-tailed testing, and other assay-specific statistical procedures are detailed in the corresponding Methods subsections. Statistical significance was defined as $P < 0.05$, with $\alpha = 0.05$.

Ethics Committee

The present study was in accordance with the NIH guidelines involving Human Subjects and for research with Animals and approved by Institutional Ethics Committees at Federal University of Rio de Janeiro, Brazil (CAAE 37520820.4.3001.5259 / CEUA UFRJ DAHEICB 053); Universidade de Ribeirão Preto (CEUA-UNAERP protocol #008/2023); Hospital Municipal Miguel Couto (CAAE 96263418.0.0000.5279), Brazil; New York Medical College (IACUC approval #69-12-0609.1), NY, and Albert Einstein College of Medicine (IACUC approval protocol #20030906), NY (*see* **SI - Ethics Statement** for details).

Role of the funding source

The sponsors of this study had no role in study design, data collection, data analysis, data interpretation, or writing of the report. C. M. Perret, T.G. de Morais, and R. Rozental had full access to all the data in the study, and all authors had final responsibility for the decision to submit for publication.

Ethics declarations

All authors declare that they have no conflict of interest

RESULTS

The companion study established an anesthesia-free model of ischemic SCI in awake rats that recapitulates key clinical, radiological, histopathological, and molecular features of human ischemic SCI while enabling high-fidelity characterization of the first 24 h after injury. Integrated multi-omic analyses identified defective engagement of endogenous inflammatory resolution, revealing only transient activation of the docosahexaenoic acid (DHA)-lipoxygenase pathway that was insufficient to prevent secondary lesion progression.

Building on these findings, we first defined the endogenous DHA-derived lipid mediator profile of the injured SC, determining which products of the HDHA biosynthetic pathway - including 7-HDHA, 14-HDHA, 17-HDHA, neuroprotectin D1, and D-series resolvins (**Fig. S2**) - are generated during the hyperacute phase of injury. We then tested whether pharmacological augmentation of the endogenous 17(S)-HDHA pathway restores inflammatory resolution, limits secondary tissue damage, modulates astroglial and macrophage responses, and improves neurological outcome following MES-induced ischemic injury of the thoracic SC in rats.

Endogenous production of 17-HDHA predominates during the hyperacute phase of ischemic spinal cord injury.

Guided by the lipidomic findings of the companion study, we next characterized the endogenous DHA-derived lipid mediator profile during the first 24 h after hindlimb paralysis **(Fig. S1),** Cerebrospinal fluid (CSF) and SC tissue collected 24 h after MES-induced injury were analyzed in a blinded manner by reverse-phase high-performance liquid chromatography coupled with diode-array detection and tandem mass spectrometry (RP-HPLC-DAD/LC–MS/MS).

Lipidomic analyses identified selective endogenous production of 17-hydroxy-docosahexaenoic acid (17-HDHA), a pathway marker for the formation of the D-series resolvins and protectin D1 (PD1) (**Fig. S2**), after injury (**Fig. 1**). RP-HPLC chromatograms revealed a peak with the characteristic retention time and conjugated diene ultraviolet chromophore of authentic 17-HDHA which was subsequently confirmed by LC–MS/MS (**Fig. 1C,G**). The major ion detected (m/z 416), together with the diagnostic fragment ion (m/z 325), was consistent with the established mass spectrometric signature of 17S-HDHA. Endogenous arachidonic acid-derived lipoxygenase products (5S-HETE, 12S-HETE, and 15S-HETE), as well as structurally related DHA metabolites (4-HDHA, 7-HDHA, and 14-HDHA), exhibited distinct chromatographic retention times and did not co-elute with 17-HDHA, confirming the specificity of its identification.

In contrast, neither 14-HDHA, a marker of the maresin biosynthetic pathway, nor downstream DHA-derived specialized pro-resolving mediators, including neuroprotectin D1 (NPD1) and D-series resolvins, were detected in SC tissue or CSF at this time point (**Fig. 1**). These findings indicate that the most abundant bioactive LOX lipid mediator generated during the hyperactive phase of injury was 17-HDHA, while other potential SPM may have been present at low levels that did not reach the detection limits of our analytical methods.

Lipidomic-based analysis employing RP-HPLC-DAD/LC–MS/MS also identified the presence of 17-HDHA in CSF in the acute phase of SCI of patients (**Fig. 1G**), strengthening the correlation between human and animal models of SC disease. These findings identify 17-HDHA as the predominant endogenous DHA-derived lipid mediator generated during the hyperacute phase of ischemic SCI.

Systemically administered 17(S)-HDHA rapidly reaches the spinal cord without detectable acute systemic toxicity

Before evaluating the neuroprotective effects of 17(S)-HDHA after ischemic SCI, we first determined whether systemically administered 17(S)-HDHA reaches SC tissue and assessed its acute systemic safety. To quantify SC biodistribution under conditions relevant to hyperacute therapeutic intervention, deuterium-labelled 17(S)-HDHA (d_5-17(S)-HDHA; 200 ng) was administered intravenously, and tissue concentrations were measured by LC–MS/MS 45 min later. Deuterium-labelled 17(S)-HDHA was readily detected throughout the thoracolumbar SC (T8–L2) (**Fig. 1H–J**), demonstrating rapid penetration into SC tissue under physiological conditions, without requiring ischemia-induced disruption of the blood–spinal cord barrier (BSCB).

Acute tolerability was subsequently evaluated using the therapeutic regimen employed throughout the study. No treatment-related mortality or adverse effects on behavior, neurological status, general clinical condition, or cardiac function were observed during the experimental period, including following intravenous administration.

To compare the systemic metabolic effects of 17(S)-HDHA with those of methylprednisolone, the corticosteroid most extensively investigated for acute SCI, serum biochemical parameters were measured 24 h after a single intravenous administration. Animals treated with 17(S)-HDHA remained normoglycemic, with serum glucose concentrations comparable to those of vehicle-treated controls (**SI Table 1**). In contrast, methylprednisolone significantly increased blood glucose concentrations (151.0 ± 8.8 vs. 184.0 ± 10.0 mg dL^{-1}, $P < 0.05$). Serum electrolyte concentrations (Na^+, K^+, Ca^{2+}, and Mg^{2+}) did not differ significantly among the experimental groups (**SI Table 1**). Together, these findings demonstrate that systemically administered 17(S)-HDHA rapidly reaches the SC and is well tolerated under the dosing regimen used in this study, without inducing the acute hyperglycemia observed following methylprednisolone administration.

17(S)-HDHA promotes inflammatory resolution, limits secondary tissue degeneration, and preserves hierarchical organization of spinal motor network recruitment despite persistent early locomotor deficits.

To determine whether the transient endogenous activation of the 17(S)-HDHA pathway could be therapeutically reinforced, 17(S)-HDHA was administered intravenously during the hyperacute (0–24 h) and acute (24–120 h) phases after the onset of paralysis. Histological, morphometric, and electrophysiological analyses were performed 5 days after injury to evaluate inflammatory responses, tissue preservation, and functional outcome.

Immunohistochemical analyses revealed that treatment with 17(S)-HDHA markedly attenuated the inflammatory response within the injured SC (**Fig. 2**). CD11b immunoreactivity was significantly reduced in peri-lesional regions compared with vehicle-treated animals ($P < 0.05$), accompanied by a shift in cellular morphology from predominantly amoeboid CD11b-positive cells in untreated animals to a more ramified phenotype with elongated processes following 17(S)-HDHA treatment. Reactive astrogliosis was similarly attenuated. Whereas vehicle-treated animals exhibited intense GFAP immunoreactivity surrounding the lesion, characterized by hypertrophic astrocytes with thickened processes, 17(S)-HDHA-treated animals displayed astrocytic morphology resembling that of uninjured tissue, with significantly reduced GFAP immunoreactivity and astrocytic hypertrophy ($P < 0.05$) (**Fig. 2**). Quantitative histological analyses confirmed significant reductions in CD11b-positive inflammatory cells together with preservation of NeuN-positive neurons in animals receiving 17(S)-HDHA (**Fig. 2P**). Collectively, these findings indicate that pharmacological augmentation of the endogenous 17(S)-HDHA pathway suppresses inflammatory cell activation while limiting reactive gliosis during the acute phase of ischemic SCI.

Histopathological examination of serial hematoxylin and eosin (H&E)-stained SC sections demonstrated the characteristic pathological features of ischemic SCI, including neuronal loss, vacuolar degeneration, inflammatory infiltrates, focal hemorrhage, and progressive tissue atrophy (**Figs. 2 and 3A,B**). Because post-ischemic tissue atrophy represented the most reproducible structural consequence of injury at day 5, lesion severity was quantified by three-dimensional reconstruction of tissue loss from serial transverse sections spanning the T8–T12 SC segments (**Fig. 3A,B**). Vacuolar degeneration was evaluated qualitatively but was not included in the volumetric analysis because variability in rostrocaudal alignment precluded reliable comparison of individual vacuolar lesions among animals.

Systemic administration of 17(S)-HDHA markedly preserved SC tissue compared with vehicle-treated animals (**Fig. 3A,B**). Untreated rats retained only 4.94 ± 1.10 mm^3 of SC tissue, corresponding to 36.7% of control values (13.48 ± 2.80 mm^3), whereas animals receiving 17(S)-HDHA retained 10.42 ± 2.00 mm^3 (77.3% of control values). One-way ANOVA demonstrated a significant treatment effect on tissue preservation ($F(2,11) = 21.28$, $P = 0.00017$). The protective effect was primarily reflected by attenuation of post-ischemic SC atrophy, indicating that 17(S)-HDHA limits secondary tissue degeneration rather than the extent of the primary ischemic insult.

Functional recovery was evaluated using complementary behavioral and electrophysiological assessments. Consistent with the severity of ischemic SCI, vehicle-treated animals developed persistent paraplegia and exhibited no significant improvement in Basso, Beattie, and Bresnahan (BBB) locomotor scores during the first 5 days after injury. Likewise, 17(S)-HDHA treatment did not significantly improve BBB scores during this early observation period. To determine whether 17(S)-HDHA preserved spinal motor circuit function despite the absence of detectable behavioral recovery, quadrifilar vector electromyography (VEMG) was performed in a total of six animals ($n = 2$ per

group), with two to three independent recordings obtained from each animal (**Fig. 2Q–S**). Representative recordings from vehicle-treated animals consistently demonstrated profound disruption of the hierarchical organization of motor unit recruitment, characterized by sparse motor unit activation, fibrillation potentials, highly synchronized discharges, and loss of the normal physiological recruitment sequence expected from intact descending motor control (**Fig. 2R**). In contrast, recordings obtained from 17(S)-HDHA-treated animals consistently demonstrated preservation of the hierarchical organization of motor unit recruitment (**Fig. 2S**). Motor units were recruited in an orderly manner consistent with the physiological size principle, exhibited asynchronous activation, maintained normal discharge-rate organization, including the characteristic onion-skin firing pattern, and displayed greater separation of motor unit firing frequencies. The temporal organization of motor unit activity closely resembled that observed in uninjured control animals (**Fig. 2Q**), indicating preservation of functional spinal motor network integrity despite persistent paralysis during the acute post-injury period. Collectively, these electrophysiological observations demonstrate preservation of the physiological organization of spinal motor output following 17(S)-HDHA treatment. Although exploratory because of the limited number of animals examined, the VEMG findings provide independent physiological validation of the behavioral, histopathological, and molecular evidence demonstrating neuroprotection, indicating that 17(S)-HDHA preserves the functional integrity of descending motor circuitry during the early phase after ischemic SCI.

17(S)-HDHA treatment attenuates Cx43 expression after ischemic spinal cord injury.

Because reactive astrocytes and inflammatory cells are major sources of connexin-43 (Cx43) after SC injury, we next examined whether the reduction in neuroinflammation induced by 17(S)-HDHA was accompanied by changes in Cx43 expression. Thoracic SC tissue (T8–T12) was collected from uninjured control rats, untreated rats, and rats treated with intravenous 17(S)-HDHA 5 days after ischemic SCI (n = 4 per group), and Cx43 protein expression was quantified by Western blot analysis (**Fig. 3C**). Untreated paralyzed animals exhibited a 24.5% increase in Cx43 protein expression relative to uninjured controls. In contrast, treatment with 17(S)-HDHA markedly attenuated Cx43 expression, reducing protein levels by 71% compared with untreated paralyzed animals and by 63% relative to controls ($P < 0.05$; **Fig. 3C**). These findings demonstrate that pharmacological augmentation of the endogenous 17(S)-HDHA pathway markedly suppresses injury-induced Cx43 upregulation during the acute phase of ischemic SCI.

DISCUSSION

Impaired resolution of inflammation is increasingly recognized as a critical determinant of outcome after SCI, yet its temporal dynamics and therapeutic relevance during acute ischemic injury remain incompletely understood[2,3,32,33]. Building directly on the companion study demonstrating early failure of inflammatory resolution after ischemic SCI, the present work identifies defective lipid-mediated resolution as a central pathogenic mechanism underlying secondary lesion progression. Specifically, we demonstrate that endogenous biosynthesis of the specialized pro-resolving mediator precursor 17-hydroxy-docosahexaenoic acid (17-HDHA) is transiently induced but insufficiently sustained after injury. Systemic administration of 17(S)-HDHA restored key components of the endogenous resolution program, attenuating inflammatory activation, limiting tissue degeneration, reducing Cx43 expression, preserving motor unit organization, and improving electrophysiological outcomes. Together, these findings establish resolution pharmacology as a promising therapeutic strategy for acute ischemic SCI.

The MES-induced ischemic SCI model reproduced several key pathological and clinical features of human ischemic SCI, including abrupt neurological deterioration, selective thoracolumbar vulnerability, progressive inflammatory infiltration, tissue vacuolization, and secondary degeneration[1,4–8]. MRI detected bilateral gray matter "owl-eyes" appearance at the lesion epicenter, suggesting a vascular ischemic nature and translational relevance of the model[1,4,5]. Histopathological analyses further revealed progressive neuronal loss, accompanied by marked reactive astrogliosis with hypertrophic GFAP-positive astrocytes surrounding the ischemic core and robust accumulation of CD11b-positive macrophages/microglia within peri-lesional regions[13,14]. These changes were associated with extensive vacuolar degeneration, increased DAPI-positive cellularity, and depletion of NeuN-positive neurons, consistent with replacement of neuronal populations by inflammatory infiltrates[13–18]. Although ischemic SCI is not primarily a hemorrhagic disorder, severe ischemia disrupted the spinal microvasculature, producing localized petechial hemorrhagic foci that colocalized with CD11b-positive inflammatory cells, increased Cx43 expression, and regions of neuronal depletion[13–18]. Collectively, these findings closely resemble human disease and indicate that vascular dysfunction, neuroinflammation, and glial activation act synergistically to drive secondary lesion expansion after ischemic SCI[14–18], providing a robust experimental platform for investigating the mechanisms of inflammatory resolution and evaluating therapeutic interventions.

A major mechanistic finding of the present study is that activation of endogenous lipid-mediated resolution occurs substantially earlier after ischemic SCI than previously recognized[9,32,34–36]. Specialized pro-resolving mediators (SPMs) derived from docosahexaenoic acid (DHA) and eicosapentaenoic acid (EPA) are now recognized as active regulators of inflammatory resolution rather than passive byproducts of inflammatory termination[2,34–36]. Whereas previous lipidomic studies in anesthetized SCI models reported activation of the resolvin and maresin pathways predominantly during later reparative stages, with 17-HDHA and 14-HDHA increasing only after approximately two weeks post-injury[9], our integrated transcriptomic, lipidomic, and protein analyses demonstrated a

transient but significant increase in endogenous 17-HDHA within the first 24 h after ischemic SCI, accompanied by upregulation of Alox15 and Alox5ap and persistent astrocytic 12/15-lipoxygenase expression. These findings indicate that inflammatory and resolution pathways are activated simultaneously during the hyperacute phase of injury rather than sequentially. Incomplete lipid mediator profile is consistent with the companion study demonstrating suppression of astrocytic programs involved in DHA transport and metabolism, including genes regulating lipid trafficking and biosynthesis, which would be expected to limit substrate availability and sustained SPM production despite activation of upstream enzymatic machinery[2]. Collectively, these findings indicate that the endogenous resolution response is initiated remarkably early after ischemic SCI but fails to progress toward complete biosynthesis of downstream pro-resolving mediators, thereby limiting effective inflammatory resolution and tissue protection.

Defective engagement of endogenous resolution pathways occurred in parallel with amplification of pro-inflammatory lipid signaling. Increased Alox5ap expression indicates activation of the 5-lipoxygenase (5-LOX)/5-LOX-activating protein (FLAP) axis, a key enzymatic pathway driving leukotriene biosynthesis and promoting leukocyte recruitment, macrophage activation, cytokine production, and secondary tissue injury[2,9,34–36]. In the companion study, this inflammatory milieu was characterized by a marked increase in MCP-1 during the first 24 h after injury, accompanied by robust accumulation of CD11b-positive inflammatory cells, whereas several canonical pro-inflammatory cytokines, including TNF-α, remained unchanged or were reduced[2]. These findings are consistent with the temporal analysis of SCI-associated cytokine regulation reported by Hellenbrand et al., who demonstrated that many classical pro-inflammatory cytokines, including TNF-α, IL-1α, and IL-1β, rapidly return toward baseline within the first 24 h after injury, whereas anti-inflammatory mediators such as IL-10, IL-4, and IL-13 remain persistently suppressed, indicating that defective inflammatory resolution rather than sustained cytokine production characterizes the evolution of secondary injury[33]. Accordingly, the continued recruitment and activation of macrophages appear to depend not solely on persistent expression of individual cytokines but also on dysregulated lipid mediator signaling and failure to engage endogenous pro-resolving pathways. Consistent with the established biological actions of specialized pro-resolving mediators, systemic administration of low-dose 17(S)-HDHA significantly attenuated macrophage accumulation and activation while preserving reparative immune responses, indicating that it promotes coordinated inflammatory resolution rather than indiscriminate immunosuppression [2,34–36]. Rather than persistent elevation of classical inflammatory cytokines alone, our findings support the concept that failure to transition from inflammation toward resolution is a major determinant of lesion progression.

An additional mechanistic insight emerging from the present study is the identification of Cx43 remodeling as a downstream consequence of defective inflammatory resolution after ischemic SCI. Although several astrocyte-enriched transcriptional signatures were markedly suppressed within the first 24 h after injury, expression of Gja1, the gene encoding Cx43, remained essentially unchanged[2]. Because astrocytes represent the principal source of Cx43 in the

healthy SC, preservation of Gja1 transcript levels despite widespread astrocytic dysfunction suggested that additional cellular populations contribute to Cx43 expression during lesion evolution. Consistent with this interpretation, Cx43 protein expression increased markedly by day 5 after injury, coinciding with robust accumulation of CD11b-positive inflammatory cells and the development of reactive astrogliosis. Infiltrating macrophages and activated microglia have been shown to express Cx43 under inflammatory conditions[14–22], while inflammatory cytokines and connexin-dependent signaling released by these cells dynamically regulate astrocytic Cx43 expression and Cx-hemichannel activity[12,37]. These observations support the concept that progressive recruitment of inflammatory myeloid cells amplifies Cx43-dependent intercellular communication within the injured SC, extending connexin signaling beyond the resident astrocytic syncytium. Because intravenously administered 17(S)-HDHA readily reached the injured SC (**Fig. 1H-J**), the marked reduction in both macrophage accumulation and Cx43 protein expression observed after treatment strongly suggests that restoration of endogenous inflammatory resolution limits expansion of this pathological signaling network. We therefore propose that defective resolution establishes a feed-forward macrophage–astrocyte inflammatory loop in which infiltrating macrophages and activated microglia sustain astrocytic Cx43 expression, while increased Cx43-mediated gap junction and hemichannel signaling further propagates inflammatory, metabolic, and injury-associated signals throughout peri-lesional tissue, thereby exacerbating secondary degeneration. In the heart, resident macrophages establish functional Cx43-dependent coupling with cardiomyocytes and directly influence electrical conduction and rhythm regulation[38]. Accumulating evidence indicates that macrophages and microglia dynamically regulate astroglial Cx43 expression through inflammatory cytokines and connexin-dependent signaling pathways [12,37]. By promoting endogenous resolution rather than broadly suppressing immune activation, 17(S)-HDHA interrupts this pathological neuroglial circuit, attenuating both inflammatory cell accumulation and Cx43 remodeling while preserving neuronal integrity and SC architecture. Collectively, these observations identify Cx43 remodeling as a downstream component of defective inflammatory resolution rather than an isolated pathogenic event.

The functional significance of these neuroprotective effects was supported by quadrifilar vector electromyographic analyses demonstrating preservation of spinal motor unit organization following 17(S)-HDHA treatment[30,31]. Although conventional BBB locomotor scores remained uniformly low during the acute post-injury period, reflecting both the severity of the ischemic lesion and the limited sensitivity of behavioral assessment during the first days after SCI, vector electromyography revealed substantial preservation of motor unit recruitment and discharge organization. Treated animals maintained orderly motor unit recruitment and the characteristic "onion-skin" firing pattern, a hallmark of physiologically intact lower motor neuron output and coordinated descending motor control[30,31]. Preservation of these electrophysiological signatures, despite profound locomotor impairment, indicates that 17(S)-HDHA stabilizes residual spinal circuitry before behavioral improvements become detectable. Together with the histopathological preservation of SC tissue and the attenuation of macrophage accumulation and Cx43 remodeling, these findings demonstrate that early restoration of inflammatory resolution preserves the functional integrity

of spinal motor networks, maintaining the neural substrate required for subsequent neurological recovery.

The translational implications of these findings are particularly relevant given that effective pharmacological therapies for acute SCI remain limited, and no intervention has yet achieved widespread clinical adoption[39–42]. Although methylprednisolone sodium succinate (MPSS) has been used for decades in the management of acute SCI, its clinical benefit remains controversial because neurological improvement is modest and inconsistent, the therapeutic window is narrow, and treatment is associated with substantial systemic adverse effects, including hyperglycemia, insulin resistance, and impaired immune function[41]. Nevertheless, recent analyses suggest that patients with the most severe cervical injuries (AIS A) derive the greatest benefit when treatment is initiated during the earliest stages of secondary injury, underscoring the importance of timely neuroprotective intervention[41]. Similarly, reanalysis of the RISCIS randomized clinical trial demonstrated that riluzole conferred the greatest therapeutic benefit in patients with severe (AIS A) SCI, while integration of multiple neurological outcome measures revealed treatment effects that were not detected by the original primary endpoint, emphasizing the complexity of assessing recovery after SCI[39]. In contrast, the phase 2b NISCI trial evaluating intrathecal anti-Nogo-A antibodies did not achieve its primary efficacy endpoint, although exploratory analyses suggested that patients with greater preservation of residual SC tissue, quantified by MRI tissue bridges, exhibited a higher probability of functional improvement following regenerative therapy[40,43]. These clinical observations closely parallel our experimental findings, in which 17(S)-HDHA preserved SC architecture, reduced macrophage accumulation and Cx43 remodeling, and maintained motor network organization during the acute phase of injury. Unlike glucocorticoids, which broadly suppress inflammatory responses, 17(S)-HDHA promotes the endogenous resolution of inflammation while preserving systemic metabolic homeostasis, thereby limiting secondary tissue degeneration without detectable corticosteroid-associated toxicity. Collectively, these studies indicate that successful treatment of SCI will likely require therapies that simultaneously preserve tissue integrity, modulate neuroinflammation, and create a permissive environment for subsequent repair.

These observations are particularly relevant because the adult mammalian SC possesses only limited regenerative capacity[44,45]. During embryonic and early postnatal development, long-distance axonal growth and target selection are orchestrated by highly coordinated gradients of attractive and repulsive guidance cues, including netrins, semaphorins, ephrins, Slits, and morphogens, which establish precise neuronal connectivity throughout the developing CNS[5]. Following maturation, however, many of these developmental programs are markedly downregulated or become functionally inactive. Consequently, after SCI, surviving axons are confronted by a profound growth-inhibitory microenvironment characterized by reactive astroglial scar formation, deposition of chondroitin sulfate proteoglycans (CSPGs), persistent neuroinflammation, and myelin-associated inhibitors such as Nogo-A, all of which markedly restrict spontaneous axonal regeneration and functional[45]. These biological constraints help explain why regenerative approaches alone have achieved only limited clinical success and underscore the importance of preserving viable SC tissue

during the hyperacute phase of injury. In this context, our findings suggest that the primary therapeutic benefit of 17(S)-HDHA is not to stimulate axonal regeneration directly, but rather to preserve the structural and cellular substrate upon which endogenous plasticity and future regenerative interventions can subsequently act. By limiting macrophage-driven secondary degeneration, promoting resolution of inflammation, and maintaining SC architecture, 17(S)-HDHA may create a more permissive microenvironment for subsequent repair, thereby complementing rather than competing with regenerative strategies such as anti-Nogo-A therapy.

In conclusion, our findings identify 17-HDHA as an endogenous mediator of the early resolution response following ischemic SCI, extending evidence that specialized pro-resolving lipid mediators actively regulate inflammation rather than simply mark its termination[2,9,32–36]. Although endogenous 17-HDHA is induced within the first 24 h after injury, this response is insufficient to sustain effective resolution. Pharmacological augmentation with intravenous 17(S)-HDHA during this hyperacute window limits secondary injury and preserves functional SC integrity. Its minimally invasive systemic delivery may enable early intervention before definitive specialized care and complement subsequent neuroprotective, reparative and regenerative strategies. This may be particularly relevant given the limited intrinsic capacity of the adult SC for structural repair[44,45] and the time-dependent loss of viable neural tissue after injury. Unlike approaches requiring direct surgical delivery or specialized hypothermic equipment[46,47], 17(S)-HDHA targets the endogenous resolution pathway through a readily deployable pharmacological intervention. Thus, rather than replacing existing or emerging therapies, 17(S)-HDHA may provide a complementary strategy to preserve the biological substrate required for their efficacy. By shifting therapeutic emphasis from broad suppression of inflammation toward enhancement of its endogenous resolution, our findings provide a translational framework for multimodal treatment of acute ischemic SCI.

ACKNOWLEDGMENTS.

We thank Drs. L. de Brito Gitirana (ICB/UFRJ) and L.A. Mattiace (Department of Cell Biology and Anatomy, New York Medical College, Valhalla, NY, USA) for assistance with histology; Dr. R. Roark (Department of Otolaryngology, New York Medical College) for electromyographic recordings and data analysis; Drs. M. Quiñones-Vega and N.D. Ortiz (Institute of Chemistry, UFRJ) for assistance with RP-HPLC; Ms. M.E. da Costa Menezes (ICB/UFRJ) for illustrations; and Drs. L.A. Alves (IOC/Fiocruz) and R.C.M. da Silva Filho (Hospital Municipal Miguel Couto, RJ) for valuable comments. This work was supported in part by the New York State Spinal Cord Injury Research Board (grant C022068, to R.R.), the Fundação Carlos Chagas Filho de Amparo à Pesquisa do Estado do Rio de Janeiro (FAPERJ; grant E-26/110.625, to R.R.), and the Brazilian Ministry of Health through grants TED 1302016-UFRJ and VPPIS 00422278-Fiocruz (to R.R.).

COMPETING INTERESTS

The authors declare no conflict of interest.

Author contributions. C.P. and T.G.M. analyzed the histological samples. C.P. and R.M.B. performed 3D spinal cord reconstruction and lesion volumetry. T.G.M. molecular biological assays. T.G.M., C.D.P., F.C.S.N. and K.G, performed lipidomic analyses of spinal cord tissue and CSF. K.G. conducted assays involving specialized pro-resolving mediators (SPMs) and provided 17(S)-HDHA. C.P., T.G.M., C.D.P and R.O.B. performed serum biochemical and metabolic safety assessments. C.P., T.G.M., K.G. and R.R. analyzed the data. R.R. wrote the manuscript.

REFERENCES

1. Tator, C. H. & Fehlings, M. G. Review of the secondary injury theory of acute spinal cord trauma with emphasis on vascular mechanisms. *J. Neurosurg.* **75**, 15–26 (1991).
2. Serhan, C. N. Pro-resolving lipid mediators are leads for resolution physiology. *Nature* **510**, 92–101 (2014).
3. Serhan, C. N., Chiang, N. & Van Dyke, T. E. Resolving inflammation: dual anti-inflammatory and pro-resolution lipid mediators. *Nat. Rev. Immunol.* **8**, 349–361 (2008).
4. Chiang, N. & Serhan, C. N. Specialized pro-resolving mediator network: an update on production and actions. *Nat. Rev. Immunol.* **20**, 753–765 (2020).
5. Serhan, C. N. *et al.* Macrophage proresolving mediator maresin 1 stimulates tissue regeneration and controls pain. *FASEB J.* **26**, 1755–1765 (2012).
6. Hong, S., Gronert, K., Devchand, P. R., Moussignac, R.-L. & Serhan, C. N. Novel docosatrienes and 17S-resolvins generated from docosahexaenoic acid in murine brain, human blood, and glial cells. *J. Biol. Chem.* **278**, 14677–14687 (2003).
7. Mukherjee, P. K., Marcheselli, V. L., Serhan, C. N. & Bazan, N. G. Neuroprotectin D1: a docosahexaenoic acid-derived docosatriene protects retinal pigment epithelial cells from oxidative stress. *Proc. Natl Acad. Sci. USA* **101**, 8491–8496 (2004).
8. Basil, M. C. & Levy, B. D. Specialized pro-resolving mediators: endogenous regulators of infection and inflammation. *Nat. Rev. Immunol.* **16**, 51–67 (2016).
9. Francos-Quijorna, I. *et al.* Maresin 1 promotes inflammatory resolution, neuroprotection and functional neurological recovery after spinal cord injury. *J. Neurosci.* **37**, 11731–11743 (2017).
10. Spray, D. C. & Bennett, M. V. L. Physiology and pharmacology of gap junctions. *Annu. Rev. Physiol.* **47**, 281–303 (1985).
11. Nagy, J. I. & Rash, J. E. Connexins and gap junctions of astrocytes and oligodendrocytes in the central nervous system. *Brain Res. Brain Res. Rev.* **32**, 29–44 (2000).
12. Takeuchi, H. & Suzumura, A. Gap junctions and hemichannels composed of connexins: potential therapeutic targets for neurodegenerative diseases. *Front. Cell. Neurosci.* **8**, 189 (2014).
13. Cronin, M., Anderson, P. N., Cook, J. E., Green, C. R. & Becker, D. L. Blocking connexin43 expression reduces inflammation and improves functional recovery after spinal cord injury. *Mol. Cell. Neurosci.* **39**, 152–160 (2008).
14. Huang, C. *et al.* Critical role of connexin43 in secondary expansion of traumatic spinal cord injury. *J. Neurosci.* **32**, 3333–3338 (2012).
15. Bennett, M. V. L., Contreras, J. E., Bukauskas, F. F. & Sáez, J. C. New roles for astrocytes: gap junction hemichannels have something to communicate. *Trends Neurosci.* **26**, 610–617 (2003).
16. Giaume, C. & McCarthy, K. D. Control of gap-junctional communication in astrocytic networks. *Trends Neurosci.* **19**, 319–325 (1996).

17. Eugenín, E. A., Eckardt, D., Theis, M., Willecke, K., Bennett, M. V. L. & Sáez, J. C. Microglia at inflammatory foci express connexin43 and functional gap junctions. *FASEB J.* **15**, 2261–2271 (2001).
18. Eugenín, E. A., Branes, M. C., Berman, J. W. & Sáez, J. C. TNF-α plus IFN-γ induce connexin43 expression and gap junction communication in human macrophages. *Proc. Natl Acad. Sci. USA* **100**, 4190–4195 (2003).
19. Spray, D. C., Ye, Z. C. & Ransom, B. R. Functional connexin hemichannels: a critical appraisal. *Glia* **54**, 758–773 (2006).
20. Sáez, J. C., Berthoud, V. M., Branes, M. C., Martínez, A. D. & Beyer, E. C. Plasma membrane channels formed by connexins: their regulation and functions. *Physiol. Rev.* **83**, 1359–1400 (2003).
21. Orellana, J. A. *et al.* ATP and glutamate released via astroglial connexin43 hemichannels mediate neuronal death through activation of pannexin1 hemichannels. *J. Neurochem.* **118**, 826–840 (2011).
22. Giaume, C., Leybaert, L., Naus, C. C. G. & Sáez, J. C. Connexin and pannexin hemichannels in brain glial cells. *Front. Pharmacol.* **4**, 88 (2013).
23. Lin, J. H. C. *et al.* Connexin mediates gap junction-independent resistance to cellular injury. *Nat. Neurosci.* **1**, 494–500 (1998).
24. Marcheselli, V. L. *et al.* Novel docosanoids inhibit brain ischemia-reperfusion-mediated leukocyte infiltration and pro-inflammatory gene expression. *J. Biol. Chem.* **278**, 43807–43817 (2003).
25. Svensson, C. I., Zattoni, M. & Serhan, C. N. Lipoxins and aspirin-triggered lipoxin inhibit inflammatory pain processing. *J. Exp. Med.* **204**, 245–252 (2007).
26. Serhan, C. N. *et al.* Resolvins: a family of bioactive products of omega-3 fatty acid transformation circuits initiated by aspirin treatment that counter proinflammation signals. *J. Exp. Med.* **196**, 1025–1037 (2002).
27. Nigam, S., Fiore, S., Luscinskas, F. W. & Serhan, C. N. The rat leukocyte-type 12-lipoxygenase exhibits an intrinsic hepoxilin A3 synthase activity. *J. Biol. Chem.* **279**, 29023–29030 (2004).
28. Gronert, K., Maheshwari, N., Khan, N., Hassan, I. R., Dunn, M. & Schwartzman, M. L. A role for the mouse 12/15-lipoxygenase pathway in promoting epithelial wound healing and host defense. *J. Biol. Chem.* **280**, 15267–15278 (2005).
29. Gronert, K., Clish, C. B., Romano, M. & Serhan, C. N. Transcellular regulation of eicosanoid biosynthesis. In: *Methods in Molecular Biology*, vol. **120**, 119–144 (Humana Press, Totowa, NJ, 1999).
30. De Luca, C. J., Gonzalez-Cueto, J. A., Bonato, P. & Adam, A. Motor unit recruitment and proprioceptive feedback decrease the common drive. *J. Neurophysiol.* **101**, 1620–1628 (2009).
31. Roark, R. M., Li, J. C., Schaefer, S. D., Adam, A. & De Luca, C. J. Multiple motor unit recordings of laryngeal muscles: the technique of vector laryngeal electromyography. *Laryngoscope* **112**, 2196–2203 (2002).
32. Serhan, C. N., Chiang, N., Dalli, J. & Levy, B. D. Specialized pro-resolving mediators in inflammation resolution. *Cold Spring Harb. Perspect. Biol.* **7**, a016311 (2015).
33. Hellenbrand, D. J. *et al.* The secondary injury cascade after spinal cord injury: an analysis of local cytokine/chemokine regulation. *Neural Regen. Res.* **19**, 1308–1317 (2024).

34. Schwab, J. M., Chiang, N., Arita, M. & Serhan, C. N. Resolvin E1 and protectin D1 activate inflammation-resolution programmes. *Nature* **447**, 869–874 (2007).
35. Buckley, C. D., Gilroy, D. W. & Serhan, C. N. Proresolving lipid mediators and mechanisms in the resolution of acute inflammation. *Immunity* **40**, 315–327 (2014).
36. Serhan, C. N., Dalli, J., Colas, R. A., Winkler, J. W. & Chiang, N. Protectins and maresins: new pro-resolving families of mediators in acute inflammation and resolution bioactive metabolome. *Biochim. Biophys. Acta* **1851**, 397–413 (2015).
37. Retamal, M. A. *et al.* Cx43 hemichannels and gap junction channels in astrocytes are regulated oppositely by pro-inflammatory cytokines released from activated microglia. *J. Neurosci.* **27**, 13781–13792 (2007).
38. Hulsmans, M. *et al.* Macrophages facilitate electrical conduction in the heart. *Cell* **169**, 510–522.e20 (2017).
39. Fehlings, M. G. *et al.* The sodium-glutamate antagonist riluzole improves outcome after acute spinal cord injury: results from the RISCIS randomised controlled trial analysed using a global statistical analytic technique. *EBioMedicine* **118**, 105863 (2025).
40. Weidner, N. *et al.* Safety and efficacy of intrathecal antibodies to Nogo-A in patients with acute cervical spinal cord injury: a randomised, double-blind, multicentre, placebo-controlled, phase 2b trial. *Lancet Neurol.* **24**, 42–53 (2025).
41. Mimura, T. *et al.* Effect of methylprednisolone in cervical spinal cord injury stratified by injury severity: analysis in 908 patients. *Spinal Cord* **64**, 177–185 (2026).
42. Kobayakawa, K. *et al.* Acute hyperglycemia impairs functional improvement after spinal cord injury in mice and humans. *Sci. Transl. Med.* **6**, 256ra137 (2014).
43. Pfyffer, D. *et al.* Prognostic value of tissue bridges in cervical spinal cord injury: a longitudinal, multicentre, retrospective cohort study. *Lancet Neurol.* **23**, 816–825 (2024).
44. Tessier-Lavigne, M. & Goodman, C. S. The molecular biology of axon guidance. *Science* **274**, 1123–1133 (1996).
45. Dickson, B. J. Molecular mechanisms of axon guidance. *Science* **298**, 1959–1964 (2002).
46. Lima, M.A.B., Menezes, K., Xerez, D.R. *et al.* Intramedullary injection of polymerized laminin in acute traumatic spinal cord injury: a first-in-human pilot study. *Spinal Cord* (2026).
47. Mensah E.O., Ghosh A., Alem A.O. *et al.* Therapeutic local hypothermia in the management of acute spinal cord injury: a systematic review and meta-analysis. *Spinal Cord* **64,** 759–767 (2026).

MAIN FIGURE LEGENDS

Fig. 1. Endogenous 17(S)-HDHA is generated in cerebrospinal fluid (CSF) after ischemic spinal cord injury (SCI) and intravenously administered 17(S)-HDHA reaches the SC of healthy rats.

(A) Reverse-phase HPLC coupled to ultraviolet diode-array detection (RP-HPLC–DAD) of synthetic 17(S)-hydroxydocosahexaenoic acid (17(S)-HDHA; 5–10 ng). The inset shows the characteristic conjugated diene ultraviolet chromophore. **(B)** LC–MS/MS spectrum of synthetic 17(S)-HDHA (1 ng), confirming its characteristic fragmentation pattern (major fragment ions shown in the inset). **(C)** RP-HPLC–DAD chromatograms (235 nm) of cerebrospinal fluid (CSF) collected from healthy rats and rats 24 h after paralysis (n = 4). A peak corresponding to the retention time of synthetic 17(S)-HDHA (arrow) was detected exclusively in CSF from injured animals. The inset shows the characteristic ultraviolet spectrum of the endogenous compound. **(D)** The endogenous peak co-eluting with synthetic 17(S)-HDHA was isolated by RP-HPLC and identified by GC/MS, confirming endogenous production of 17(S)-HDHA after ischemic SCI. **(E–G)** Detection of endogenous 17(S)-HDHA in CSF from patients with ischemic SCI (n = 2). **(E)** RP-HPLC chromatogram of control CSF spiked with deuterium-labelled 17(S)-HDHA (d_5-17(S)-HDHA). **(F)** Co-elution of deuterated and endogenous 17(S)-HDHA confirms identical chromatographic retention times. **(G)** Representative chromatogram demonstrating endogenous 17(S)-HDHA in CSF from a patient with ischemic SCI, corroborating the findings obtained in the rat model. **(H–J)** Biodistribution of systemically administered 17(S)-HDHA. Healthy rats received a single intravenous bolus of deuterium-labelled 17(S)-HDHA (d_5-17(S)-HDHA), and thoracolumbar SC tissue was analyzed 45 min later by LC–MS/MS (n = 3 rats). Detection of both endogenous and deuterium-labelled 17(S)-HDHA within SC tissue demonstrates rapid penetration of circulating 17(S)-HDHA into the SC under physiological conditions, indicating that tissue access does not require prior ischemic disruption of the blood–spinal cord barrier.

Fig. 2. 17(S)-HDHA attenuates neuroinflammation, preserves spinal cord architecture, and improves spinal motor network function after ischemic spinal cord injury.

(A–E) Representative transverse sections of the T10 spinal SC from uninjured rats stained with hematoxylin and eosin (H&E) (**A**), GFAP (**B**), CD11b (**C**), NeuN (**D**), and DAPI (**E**), illustrating normal SC cytoarchitecture. **(F–J)** Sections obtained 5 days after MES-induced ischemic SCI from untreated rats, showing severe tissue atrophy, disruption of SC architecture, vacuolar degeneration, neuronal loss, displacement of the central canal, reactive astrogliosis, increased CD11b immunoreactivity, and inflammatory cell infiltration. **(K–O)** Sections from rats treated with 17(S)-HDHA, demonstrating marked preservation of SC architecture, reduced tissue degeneration, attenuation of reactive astrogliosis and CD11b-positive inflammatory cell accumulation, and increased neuronal preservation relative to untreated animals. The scale bar in **N** applies to all histological panels: 500 µm (**A,F,K**); 250 µm (**B,G,L)**, 125 µm (**C,H,M)**, 50 µm (**D,E,I,J,N,O**). **(P)** Quantification of NeuN-positive neurons, GFAP-positive astrocytes, and CD11b-positive inflammatory cells. Four to five non-overlapping microscopic fields were analyzed per animal from adjacent sections stained with NeuN, GFAP, CD11b, and DAPI (n = 4 rats per group). Data are expressed as cell density (cells mm^{-2}) and presented as mean ± SD. Statistical significance was determined by one-way ANOVA followed by Tukey's multiple-comparisons test. **(Q–S)** Representative quadrifilar vector electromyographic (EMG) recordings from hindlimb muscles. **(Q)** Control rat showing physiological recruitment of multiple motor units (MUs), complex motor unit action potentials, and coordinated modulation of firing rates. **(R)** Untreated rat 5 days after ischemic SCI exhibiting sparse motor unit recruitment, fibrillation potentials, and highly synchronized firing patterns consistent with disrupted descending motor control and predominantly reflex-mediated spinal activity. **(S)** Rat treated with 17(S)-HDHA showing improved motor unit recruitment, preservation of the physiological "onion-skin" firing pattern, greater separation of motor unit firing rates, and reduced cross-covariance among active motor units, consistent with improved spinal motor network organization.

Fig. 3. 17(S)-HDHA limits secondary tissue degeneration and reduces connexin-43 (Cx43) expression after ischemic spinal cord injury.

(A) Representative hematoxylin and eosin (H&E)-stained transverse SC sections illustrating the three-dimensional morphometric approach used to quantify lesion volume. Tissue atrophy and lesion boundaries were delineated from serial sections and reconstructed volumetrically. Compared with vehicle-treated rats (*n* = 5), animals treated with 17(S)-HDHA (*n* = 4) exhibited reduced tissue atrophy, diminished vacuolar degeneration, and greater preservation of SC architecture. Representative three-dimensional reconstructions are shown, with glial scar tissue depicted in pink and vacuolated regions in light blue. Scale bar 2,400 μm. **(B)** Quantification of lesion volume reconstructed from serial histological sections. Treatment with 17(S)-HDHA significantly reduced lesion volume compared with vehicle-treated animals. Data are presented as mean ± SD (*n* = 5 vehicle; *n* = 4 17(S)-HDHA). Statistical analysis was performed using one-way ANOVA followed by Tukey's multiple-comparisons test. $P < 0.05$. **(C)** Representative immunoblots and densitometric analysis of Cx43 expression in thoracic SC tissue (T8–T12) collected 5 days after ischemic SCI. Cx43 protein levels were markedly increased in vehicle-treated animals and significantly reduced following 17(S)-HDHA treatment. Densitometric values were normalized to the corresponding β-actin loading control and are presented as mean ± SD (*n* = 4 rats per group). Statistical analysis was performed using one-way ANOVA followed by Tukey's multiple-comparisons test. $P < 0.05$.

Figures

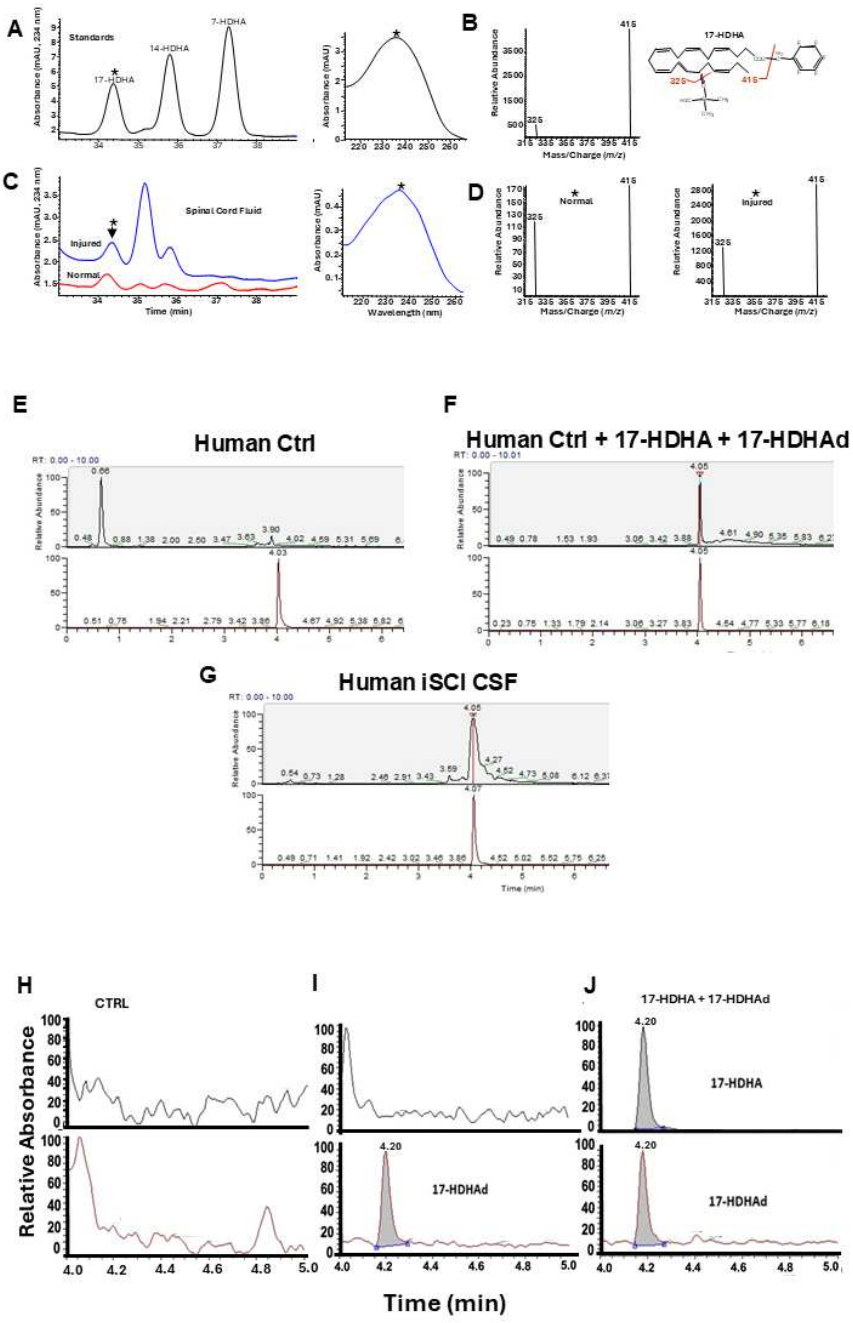
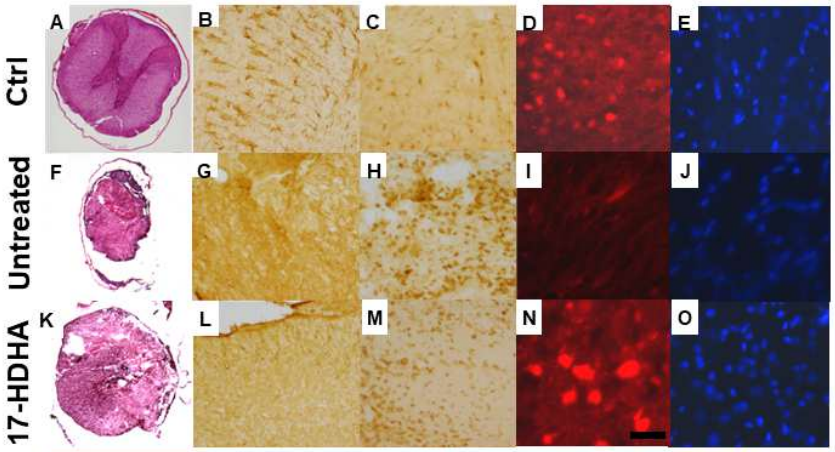


Figure 1

Endogenous 17(S)-HDHA is generated in cerebrospinal fluid (CSF) after ischemic spinal cord injury (SCI) and intravenously administered 17(S)-HDHA reaches the SC of healthy rats.

(A) Reverse-phase HPLC coupled to ultraviolet diode-array detection (RP-HPLC–DAD) of synthetic 17(S)-hydroxydocosahexaenoic acid (17(S)-HDHA; 5–

10 ng). The inset shows the characteristic conjugated diene ultraviolet chromophore. **(B)** LC–MS/MS spectrum of synthetic 17(S)-HDHA (1 ng), confirming its characteristic fragmentation pattern (major fragment ions shown in the inset). **(C)** RP-HPLC–DAD chromatograms (235 nm) of cerebrospinal fluid (CSF) collected from healthy rats and rats 24 h after paralysis (*n* = 4). A peak corresponding to the retention time of synthetic 17(S)-HDHA (arrow) was detected exclusively in CSF from injured animals. The inset shows the characteristic ultraviolet spectrum of the endogenous compound. **(D)** The endogenous peak co-eluting with synthetic 17(S)-HDHA was isolated by RP-HPLC and identified by GC/MS, confirming endogenous production of 17(S)-HDHA after ischemic SCI. **(E–G)** Detection of endogenous 17(S)-HDHA in CSF from patients with ischemic SCI (*n* = 2). **(E)** RP-HPLC chromatogram of control CSF spiked with deuterium-labelled 17(S)-HDHA (d_5-17(S)-HDHA). **(F)** Co-elution of deuterated and endogenous 17(S)-HDHA confirms identical chromatographic retention times. **(G)** Representative chromatogram demonstrating endogenous 17(S)-HDHA in CSF from a patient with ischemic SCI, corroborating the findings obtained in the rat model. **(H–J)** Biodistribution of systemically administered 17(S)-HDHA. Healthy rats received a single intravenous bolus of deuterium-labelled 17(S)-HDHA (d_5-17(S)-HDHA), and thoracolumbar SC tissue was analyzed 45 min later by LC–MS/MS (*n* = 3 rats). Detection of both endogenous and deuterium-labelled 17(S)-HDHA within SC tissue demonstrates rapid penetration of circulating 17(S)-HDHA into the SC under physiological conditions, indicating that tissue access does not require prior ischemic disruption of the blood–spinal cord barrier.



P

GROUP (n=4) STAINING	CONTROL pxl (%) /10^4	UNTREATED pxl (%)/10^4	17(S)-HDHA pxl (%)/10^4
CD11b (n=4)	130 ± 13.5 (7.5%)	458 ± 42 (36%)*	356 ± 35 (27%) *
GFAP (n-5)	128 ± 13 (14%)	60 ± 6 (11%)	56 ± 6 (10%)
NeuN (n=4)	12 ± 2 (21%)	1 ± 0.2 (1.7%) *	10 ± 1.5 (17.5%)
DAPI (n=5)	61 ± 6 (25%)	50 ± 5 (21%)	55 ± 5 (22.5%)
RATIO	1 : 11 : 11	1 : 60 : 458	1 : 6 : 36
Neurons : Astrocytes: Inflammatory Cells CD11b+			

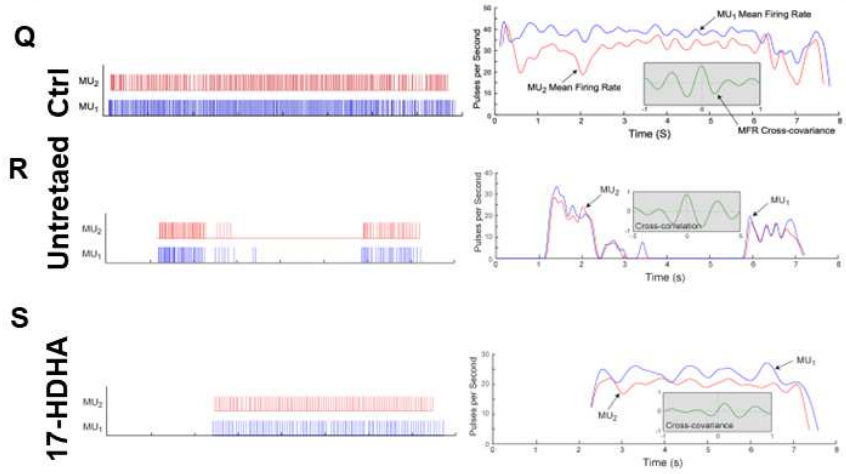


Figure 2

17(S)-HDHA attenuates neuroinflammation, preserves spinal cord architecture, and improves spinal motor network function after ischemic spinal cord injury.

(A–E) Representative transverse sections of the T10 spinal SC from uninjured rats stained with hematoxylin and eosin (H&E) (**A**), GFAP (**B**), CD11b (**C**), NeuN (**D**), and DAPI (**E**), illustrating normal SC

cytoarchitecture. **(F–J)** Sections obtained 5 days after MES-induced ischemic SCI from untreated rats, showing severe tissue atrophy, disruption of SC architecture, vacuolar degeneration, neuronal loss, displacement of the central canal, reactive astrogliosis, increased CD11b immunoreactivity, and inflammatory cell infiltration. **(K–O)** Sections from rats treated with 17(S)-HDHA, demonstrating marked preservation of SC architecture, reduced tissue degeneration, attenuation of reactive astrogliosis and CD11b-positive inflammatory cell accumulation, and increased neuronal preservation relative to untreated animals. The scale bar in **N** applies to all histological panels: 500 µm (**A,F,K**); 250 µm (**B,G,L)**, 125 µm (**C,H,M)**, 50 µm (**D,E,I,J,N,O**). **(P)** Quantification of NeuN-positive neurons, GFAP-positive astrocytes, and CD11b-positive inflammatory cells. Four to five non-overlapping microscopic fields were analyzed per animal from adjacent sections stained with NeuN, GFAP, CD11b, and DAPI (*n* = 4 rats per group). Data are expressed as cell density (cells mm^{-2}) and presented as mean ± SD. Statistical significance was determined by one-way ANOVA followed by Tukey's multiple-comparisons test. **(Q–S)** Representative quadrifilar vector electromyographic (EMG) recordings from hindlimb muscles. **(Q)** Control rat showing physiological recruitment of multiple motor units (MUs), complex motor unit action potentials, and coordinated modulation of firing rates. **(R)** Untreated rat 5 days after ischemic SCI exhibiting sparse motor unit recruitment, fibrillation potentials, and highly synchronized firing patterns consistent with disrupted descending motor control and predominantly reflex-mediated spinal activity. **(S)** Rat treated with 17(S)-HDHA showing improved motor unit recruitment, preservation of the physiological "onion-skin" firing pattern, greater separation of motor unit firing rates, and reduced cross-covariance among active motor units, consistent with improved spinal motor network organization.

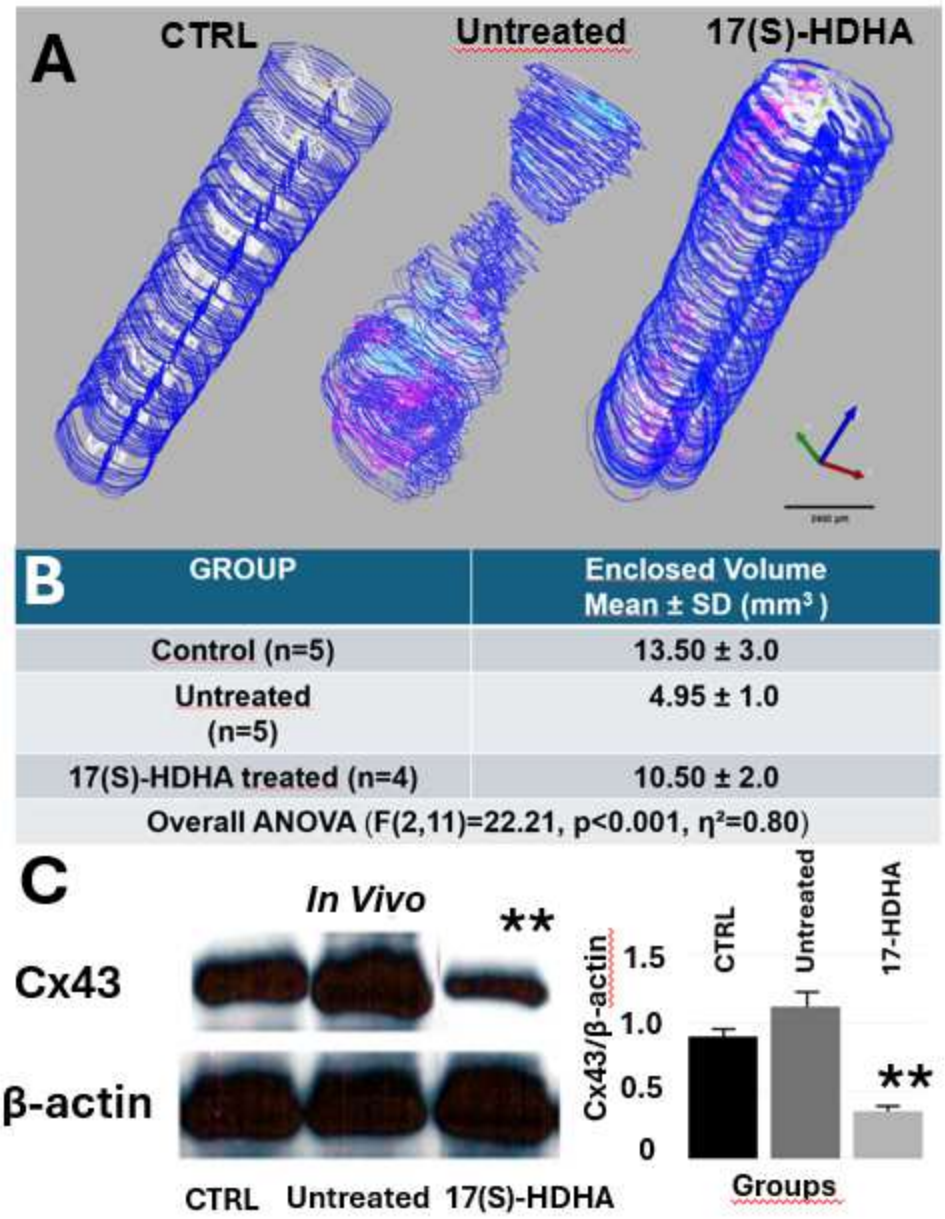


Figure 3

17(S)-HDHA limits secondary tissue degeneration and reduces connexin-43 (Cx43) expression after ischemic spinal cord injury.

(A) Representative hematoxylin and eosin (H&E)-stained transverse SC sections illustrating the three-dimensional morphometric approach used to quantify lesion volume. Tissue atrophy and lesion boundaries were delineated from serial sections and reconstructed volumetrically. Compared with vehicle-treated rats (*n*

= 5), animals treated with 17(S)-HDHA (*n* = 4) exhibited reduced tissue atrophy, diminished vacuolar degeneration, and greater preservation of SC architecture. Representative three-dimensional reconstructions are shown, with glial scar tissue depicted in pink and vacuolated regions in light blue. Scale bar 2,400 µm.

(B) Quantification of lesion volume reconstructed from serial histological sections. Treatment with 17(S)-HDHA significantly reduced lesion volume compared with vehicle-treated animals. Data are presented as mean ± SD (*n* = 5 vehicle; *n* = 4 17(S)-HDHA). Statistical analysis was performed using one-way ANOVA followed by Tukey's multiple-comparisons test. $P < 0.05$. **(C)** Representative immunoblots and densitometric analysis of Cx43 expression in thoracic SC tissue (T8–T12) collected 5 days after ischemic SCI. Cx43 protein levels were markedly increased in vehicle-treated animals and significantly reduced following 17(S)-HDHA treatment. Densitometric values were normalized to the corresponding β-actin loading control and are presented as mean ± SD (*n* = 4 rats per group). Statistical analysis was performed using one-way ANOVA followed by Tukey's multiple-comparisons test. $P < 0.05$.

Supplementary Files

This is a list of supplementary files associated with this preprint. Click to download.

- MANUSCRIPTN210152026SIMATERIALLNrr.pdf